1    **Functional assessment of the ionotropic receptors IR25a and IR93a in**

2    **predator perception in the freshwater crustacean *Daphnia* using RNA**

3    **interference**

4    Graeve A[1], Huster J[1], Mayweg J[1], Fiedler R[1], Plaßmann J[1], Wahle, P [2], Weiss LC[1]

5    [1]Department of Animal Ecology, Evolution and Biodiversity, Faculty of Biology and

6    Biotechnology, Ruhr-University Bochum, Universitätsstrasse 150, 44780 Bochum, Germany

7    [2] Department of Developmental Neurobiology, Faculty of Biology and Biotechnology, Ruhr-

8    University Bochum, Universitätsstrasse 150, 44780 Bochum, Germany

9

10    **Corresponding author**

11    Dr. Linda C. Weiss, Department of Animal Ecology, Faculty of Biology and Biotechnology,

12    Ruhr-University Bochum, Universitätsstrasse 150, 44780 Bochum, Germany, Phone: +49 234

13    32 25072, E-mail: Linda.Weiss@rub.de

14

15    **Abstract**

16    Acquiring environmental information is vital for organisms as it informs about the location of

17    resources, mating partners, and predators. The freshwater crustacean *Daphnia* detects predator

18    specific chemical cues released by its predators and subsequently develops defensive

19    morphological features that reduce the predation risk. The detection of such chemical

20    information is generally processed via distinct chemoreceptors that are located on

21    chemoreceptor cells. Lately an ancestral type of ionotropic receptors (IRs) has been identified

22    in crustaceans. IRs and the putative co-receptors IR25a and IR93a are postulated to be involved

23    in chemoreception However, functional roles have not been assessed. Here, using three

24    *Daphnia* species as model, we report that the two co-receptors are expressed within the

25  chemosensory antennules and gene expression is increased with predator perception.

26  Importantly, RNA interference mediated knock-down of the two IRs impedes species-specific

27  defense expression in the three *Daphnia* species. Our results suggest that (albeit not testing the

28  enigmatic receptor protein directly), the reduction of two associated proteins has impaired the

29  functional aggregation of the postulated chemoreceptor complex. This in turn has hampered the

30  perception of environmentally relevant chemical cues resulting in a substantial reduction of

31  defensive morphological features.

32

## Introduction

34  In aquatic systems trophic interactions greatly rely on chemical signaling. Chemical cues

35  deliver information on presence of mating partners, location of food sources and even optimal

36  breeding grounds (Pohnert, Steinke, and Tollrian 2007; Wisenden 2000; Hay 2009; Atema

37  1988). Furthermore, chemical cues inform about the presence and activity of predators which

38  in the prey can elicit defensive strategies (Tollrian and Harvell 1999). These defenses include

39  shifts in life history parameters, alternative behavioral patterns (such as seeking refuge), or the

40  expression of morphological defense structures imposing handling difficulties on predators.

41  Until now, we have limited knowledge on the nature of the chemical cues (Weiss et al. 2018;

42  Pijanowska et al. 2020; Yasumoto et al. 2005; Selander et al. 2015; Hahn et al. 2019). Even less

43  is known about the chemoreceptive mechanisms involved in interspecific information transfer.

44  The micro-crustacean *Daphnia* is an important component of freshwater food webs. The

45  different *Daphnia* species display strong phenotypic plasticity against a range of predator-

46  specific chemical cues. These cost-benefit optimized defense strategies increase organism

47  fitness (Weiss and Tollrian 2018). For example, fatty acids conjugated to a glutamine residue

48  are released from the phantom midge larva *Chaoborus*, and induce neckteeth expression in *D.*

49    *pulex* (Krueger and Dodson, 1981; Tollrian, 1993; Weiss et al., 2016). Fish-specific bile salts

50    (5-alpha-cyprinol) induce head- and tail-spine development in *D. lumholtzi* (Hahn & von Elert,

51    2022). *D. magna* reacts to fish cues by diel vertical migration (Ringelberg 2010). Cues released

52    by the tadpole shrimp *Triops* trigger *D. magna* to grow larger and bulkier (Rabus and Laforsch

53    2011). Cues released from *Triops* initiate in *D. barbata* a conspicuous helmet formation and a

54    change in body symmetry. In response to cues released by the heteropteran backswimmer

55    *Notonecta, D. barbarta* expresses a helmet that differs in shape from that induced by *Triops*

56    exposure (Herzog and Laforsch 2013). In *D. longicephala, Notonecta*-specific cues induce

57    crests (Grant and Bayly, 1981; Weiss et al., 2015). This diversity of adaptive responses shows

58    that *Daphnia* distinguish their predators based on the chemical composition of the signaling

59    agents, and confirm the view that defense morphologies are species-specific responses to

60    specifically impose handling problems for a selected predator.

61    In order to detect these sometimes highly complex compounds at extremely low concentrations

62    (in the range of nano- or even picograms (Hahn et al. 2019; Weiss et al. 2018)) *Daphnia* need

63    a chemoreceptive sensory system with specific chemoreceptors. Putative chemoreceptor

64    candidates belong to a group of ligand-gated ion channels (ionotropic receptors, IRs) that

65    evolved from ionotropic glutamate receptors (iGluRs) (reviewed in Derby et al. 2016; Benton

66    2015; Robertson 2015; Joseph and Carlson 2015; Zufall and Munger 2016). IRs are conserved

67    across Protostomia including e.g. chelicerates (Rytz, Croset, and Benton 2013), myriapods

68    (Kenny et al. 2015) and crustaceans (Eyun et al. 2017; Kozma et al. 2018; Croset et al. 2010;

69    Derby et al. 2016). Within this class of ligand-gated ion channels, IRs are classified as tuning

70    IRs and co-receptor IRs. Tuning IRs are ligand-specific and crucial for receptor channel

71    function (Benton et al. 2009; Croset et al. 2010; Rytz, Croset, and Benton 2013; Eyun et al.

72    2017) and, given the diversity of potential ligands, presumably are highly diverse. Co-receptor

73    IRs are co-expressed as heterotetramers associated with the tuning IRs, and are highly

74    conserved across taxa. Co-receptor IRs have been identified in various crustaceans (Hollins et

75    al. 2003; Corey et al. 2013; Groh et al. 2014; Zbinden et al. 2017; Groh-Lunow et al. 2015;

76    Eyun et al. 2017). In the spiny lobster *Panulirus argus* four co-receptor IRs have been identified

77    in the transcriptome: IR8a, IR25a, IR76b, and IR93a. The IR25a has even been shown to be

78    functionally involved in chemoreception in the salmon louse *Lepeophtheirus salmonis*. RNAi

79    mediated knock down of IR25a changes the louse' sensitivity to the salmon host (Núñez-Acuña

80    et al. 2019).

81    Genome data have revealed that *Daphnia pulex* has a comparatively high number of

82    chemoreceptors among which are 58 receptors that share sequence homology to the gustatory

83    receptor family of insects (Pẽnalva-Arana, Lynch, and Robertson 2009). About 150 iGluR-

84    derived IRs and three co-IRs, IR76b, IR93a and IR25a, have been identified *in silico* (Kozma,

85    Ngo-Vu, Yan Wong, et al. 2020). However, the functional expression of these IRs and the co-

86    IRs in *Daphnia* has not been investigated, and it is unknown whether they are functionally

87    involved in chemoreception. Such a functional involvement could be seen in tissue-specific

88    expression. The organ involved in predator perception was previously identified as the

89    aesthetascs of the antennules (Weiss, Leimann, and Tollrian 2015), so that these receptors are

90    hypothesized to be predominantly expressed in sensory organs such as the antennules. Further,

91    the time- and environment-dependent expression changes are unknown. The functional

92    importance of the co-IRs renders them attractive targets for experimental manipulation. Here,

93    we studied in three *Daphnia* species (*D. longicephala*, *D. magna*, *D. lumholtzi*) the expression

94    of the two co-IR genes *IR25a* and *IR93a*, determined the expression changes upon exposure to

95    chemical cues released from three predators (*Notonecta* spec.*, Triops* spec., three-spined

96    stickleback *Gasterosteus aculeatus)*, and report that co-IR RNAi impairs the expression of

97    species-specific defense morphologies.

98

## Results

### Co-receptor IR expression levels in the antennules, body and swimming antennae

We found a higher abundance of IR25a and IR93a mRNA in the antennules compared to the rest of the body (fig. 1 A, tab. 1). IR25a is 3.54 log2-fold higher expressed in the antennules than in the swimming antennae, while IR93a is 1.64 log2-fold higher expressed in the antennules than in the swimming antennae (fig. 1 B, tab. 1). IR25a is 4.28 log2-fold higher expressed in the antennules than in the body, while IR93a is 2.12 log2-fold higher expressed in the antennules than in the body. Both receptors are low but significantly higher expressed in the swimming antennae in comparison to the body with 0.74 log2-fold for the IR25a and 0.9 for the IR93a (fig. 1 C, tab. 1).
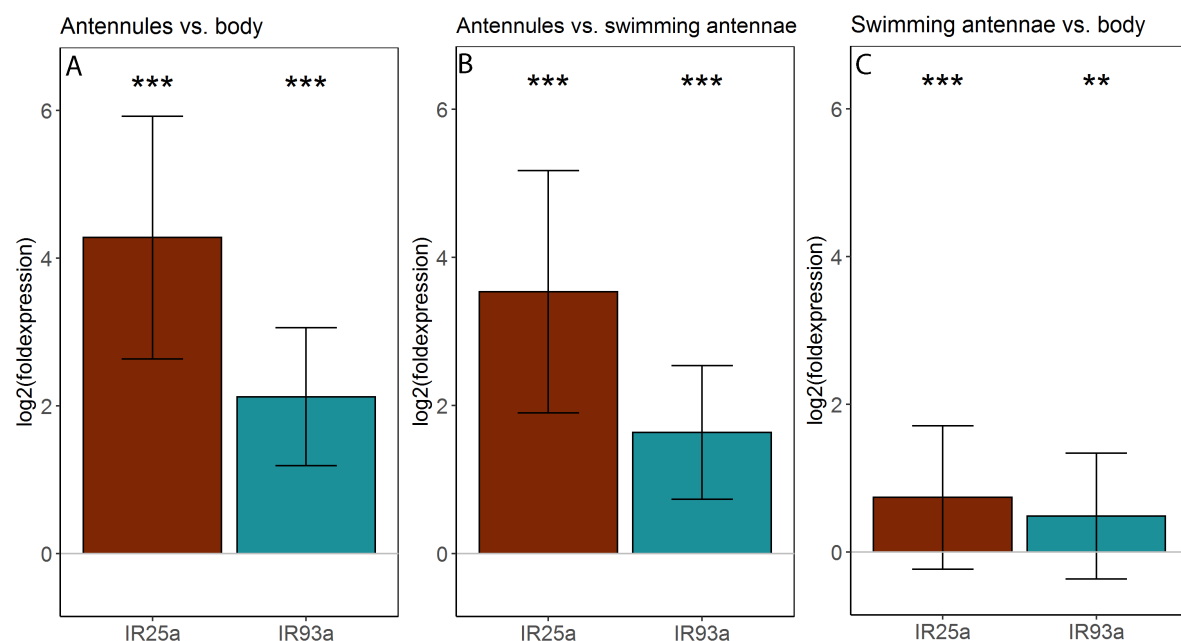


**Figure 1: Comparative co-receptor IR expression levels in different tissues of *D. longicephala*.** **A**: Increased gene expression of IR25a and IR93a in the antennules compared to the body (log2(fold expression). Both genes are significantly higher expressed in the antennules than in the body. **B:** Comparative gene expression analysis of the IR25a and the IR93a log2(fold expression) in the antennules compared to the swimming antennae. Both genes are significantly more expressed in the antennules than in the swimming antennae. **C:** Comparative gene expression analysis of the IR25a and the IR93a log2(fold expression) in the

5

118    swimming antennae compared to the body. Genes are not significantly higher expressed in the
119    swimming antennae in comparison to the body. Statistical results for one-sided T-tests are
120    displayed in tab. 1. Bar heights depicts the mean, whiskers display ± standard deviation.
121

122    **Table 1: Comparative gene expression analysis of IR gene in different tissues in _D._**
123    **_longicephala_.** T-test results of data displayed in figure 1.

| Tissue comparison | gene | Estimate | T-value | _P_-value | _N_ |
|---|---|---|---|---|---|
| Antennules vs. body | IR25a | 4.28 | 13.8 | <0.001 | 28 |
| Antennules vs. body | IR93a | 2.12 | 12.03 | <0.001 | 28 |
| Antennules vs. swimming antennae | IR25a | 3.54 | 11.43 | <0.001 | 28 |
| Antennules vs. swimming antennae | IR93a | 1.64 | 9.61 | <0.001 | 28 |
| Swimming antennae vs. body | IR25a | 0.74 | 4.04 | <0.001 | 28 |
| Swimming antennae vs. body | IR93a | 0.49 | 3.04 | <0.01 | 28 |

124
125


126    **Time series of predator induced differential IR25a and IR93a gene expression**

127    We determined the IR25a and IR93a receptors' expression levels in a time series after predator

128    exposure and compared it to control animals. While gene expression patterns are low and lie

129    around 0-log2-fold during the first 4 h, it significantly increases 6 hours after predator exposure

130    reaching a maximum expression of 1.5 log2-fold in the IR25a and 1.21 log2-fold in the IR93a.

131    Both receptors maintain an upregulated level until 24 h (fig. 2, tab. 2).
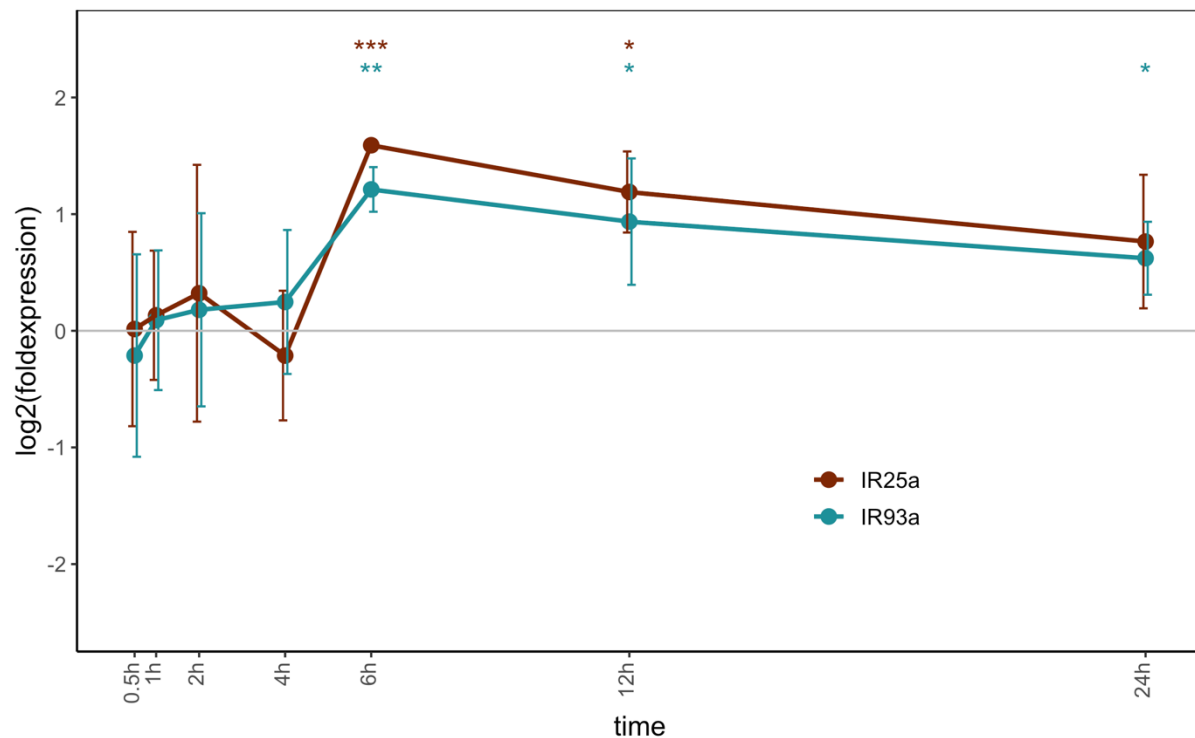
132

133

6

**Figure 2:** Time series of IR gene expression comparing gene expression levels of IR25a and IR93a in predator-exposed animals in comparison to control animals. IR25a gene expression is significantly up-regulated 6 h and 12 h and with a tendency at 24 h (p=0.07) post predator exposure. IR93a is significantly upregulated 6 h, 12 h and 24 h post predator exposure. Statistical results are displayed in table 2.

**Table 2:** Differential gene expression statistical analysis results comparing control and predator exposed *D. longicephala* over the measured points in time, as displayed in figure 2.

| time | gene | Mean | T-value | *P*-value | *N* |
|------|------|------|---------|-----------|-----|
| 0.5h | IR25a | 0.02 | 0.03 | 0.489 | 3 |
| 0.5h | IR93a | -0.21 | -0.42 | 0.643 | 3 |
| 1h | IR25a | 0.13 | 0.54 | 0.310 | 5 |
| 1h | IR93a | 0.09 | 0.34 | 0.376 | 5 |
| 2h | IR25a | 0.32 | 1.09 | 0.14 | 14 |
| 2h | IR93a | 0.17 | 0.81 | 0.21 | 14 |
| 4h | IR25a | -0.21 | -0.66 | 0.712 | 3 |
| 4h | IR93a | 0.25 | 0.69 | 0.280 | 3 |
| 6h | IR25a | 1.59 | 120.21 | <0.001 | 3 |
| 6h | IR93a | 1.21 | 10.98 | 0.004 | 3 |
| 12h | IR25a | 1.19 | 5.93 | 0.014 | 3 |
| 12h | IR93a | 0.94 | 2.99 | 0.048 | 3 |
| 24h | IR25a | 0.77 | 2.31 | 0.073 | 3 |
| 24h | IR93a | 0.62 | 3.45 | 0.037 | 3 |

7

146

**RNAi dependent knock down of predator induced morphological defenses**

To study the effect of dsRNAi probes (i.e. eGFP dsIR25a, dsIR93a) we performed a full-factorial analysis of the different treatment groups (fig. 3, tab. S1, S2). eGFP-probe injected *D. longicephala* show a significantly larger relative crests height upon predator exposure in comparison to animals of the control condition. *D. longicephala* injected with dsIR25a do not show significant differences in relative crest height between the control and the predator exposed animals but are significantly smaller in comparison to the eGFP-induced group. Similarly, when injected with the dsIR93a-probe, relative crest height in predator exposed animals is not significantly different from the controls but still share similarities with the eGFP-induced group. (fig. 3 A, tab. S1, S2). This result is supported by a significant down regulation of both genes in the IR injected specimens in comparison to the eGFP injected specimens (fig. 3 B, tab. S3).

eGFP-probe injected *D. magna* show significantly increased body width upon predator exposure in comparison to animals of the control condition. *D. magna* injected with dsIR25a do not show significant differences in body width between the control and the predator exposed group but are significantly smaller in comparison to the eGFP-induced group. Similarly, when injected with the dsIR93a-probe, body width is not significantly different from the controls in predator exposed animals but significantly smaller in comparison to the eGFP-induced group (fig. 3 C, tab. S1, S2). This result is supported by a significant down regulation of both genes in the IR injected specimens in comparison to the eGFP injected specimens (fig. 3 D, tab. S3).

Both *D. lumholtzi* LA2 *and* TE clones show a significant predator dependent increase in relative head spine length when injected with the eGFP-probe. *D. lumholtzi* injected with dsIR25a do not show significant differences in relative head spine length between the control and the predator exposed animals but have significantly smaller head spines than the eGFP-induced

171     group. Similarly, when injected with the dsIR93a-probe, relative head spine length is not

172     significantly different from the controls but significantly smaller when compared to the eGFP-

173     induced group (fig.3 E, G, F tab. S1, S2). This result is supported by a significant down

174     regulation of both genes in the IR injected specimens in comparison to the eGFP injected

175     specimens (fig. 3 B, tab. S3).

176     We repeated this experiment with alternative RNAi probes and found the same effects in the

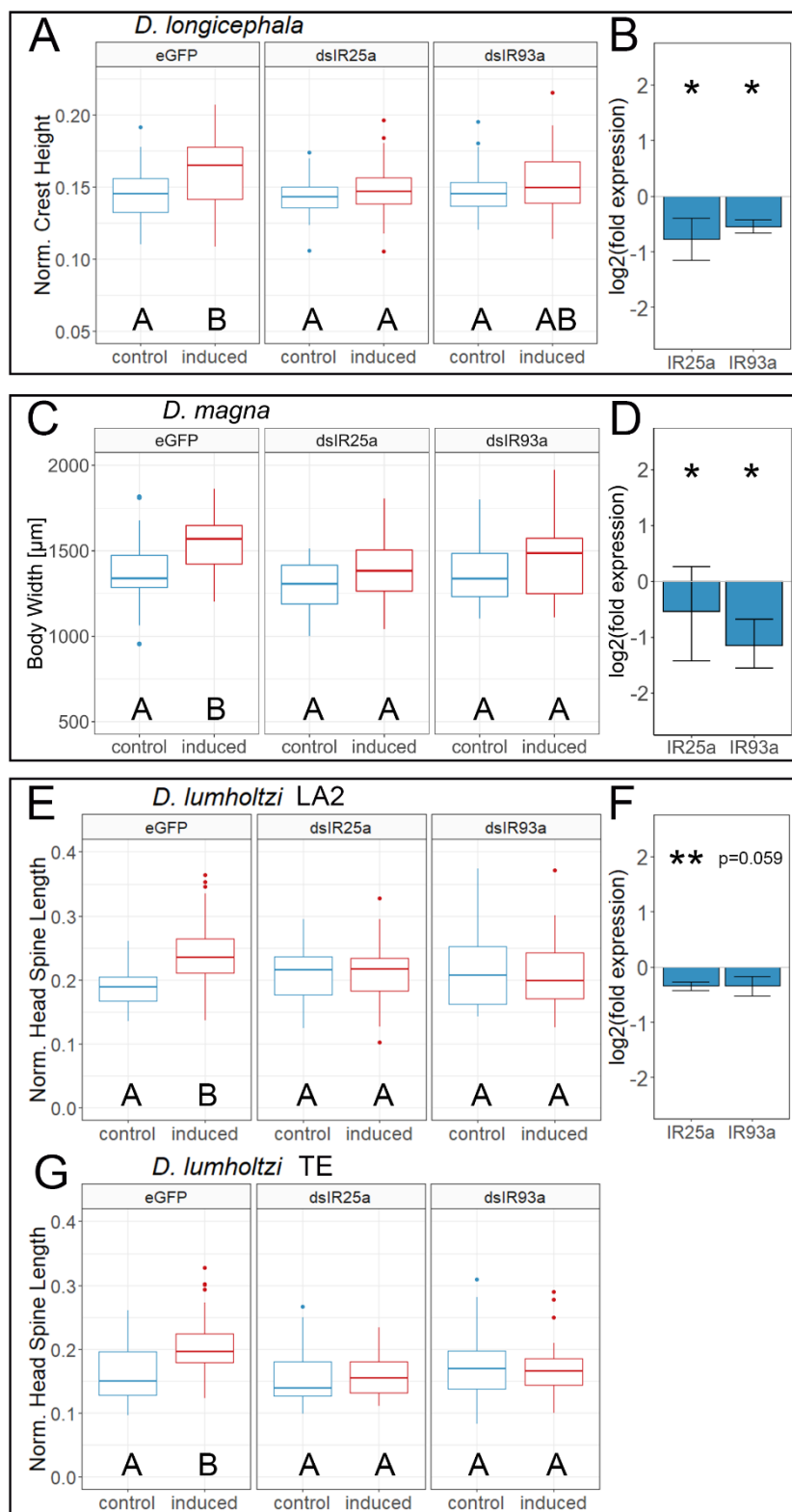177     morphology of the animals (fig. 4, tab S5, S6).

9

178

**Figure 3: Morphological defense expression upon predator exposure after micro-injection with eGFP-, dsIR25a- or dsIR93a-probe. A**: Normalized crest height of *D. longicephala*

181    exposed to *Notonecta* spec. after injection with eGFP-, dsIR25a- or dsIR93a-probe. Predator
182    exposure after eGFP-probe injection have significantly larger crests compared to the control
183    treatment. Individuals injected with dsIR25a- or dsIR93a-probe do not express increased crest
184    heights compared to the controls. Predator exposed dsIR93a injected *D. longicephala* injected
185    with express crests that reach the level of the eGFP predator exposed animals. **B:** log2(fold
186    expression) of IR25a and IR93a after probe injection. IR25a is significantly downregulated
187    upon probe injection (log2(fold expression) = -0.77, t=-2.053, *P*=0.03). IR93a is with -0.55-
188    log2fold significantly down regulated after probe injection, (t=-4.6, *P*=0.022). **C:** Body width
189    of *Triops* spec exposed *D. magna* injected with eGFP-, dsIR25a- or dsIR93a-probe. Predator
190    exposure after eGFP-probe injection induces defense significantly. Individuals injected with
191    dsIR25a- or dsIR93a-probe do not express defensive features. **D:** log2(fold expression) of
192    *IR25a* and *IR93a* after probe injection in *D. magna*. Both IRs are significantly downregulated
193    upon injection with the respective probe (IR25a log2(fold expression) = -0.44, t=-2.4, *P*=0.037;
194    IR93a: log2(fold expression) = -0.96, t=-2.79, *P*=0.025). **E:** Normalized head spine length of
195    *D. lumholtzi* clone LA2 exposed to *Gasterosteus aculeatus* after injection with eGFP-,
196    dsIR25a- or dsIR93a-probe. Predator exposure after eGFP-probe injection induces defenses
197    significantly. Individuals injected with dsIR25a- or dsIR93a-probe do not express head spines.
198    **F:** log2(fold expression) of IR25a and IR93a in *D. lumholtzi* LA2 after probe injection. IR25a
199    is significantly downregulated (IR25a: log2(fold expression) = -0.35, t=-4.4, *P*=0.006), IR93a
200    has a tendency to a downregulation after injection with the dsIR93a-probe (IR93a: log2(fold
201    expression) = -0.35, t=-1.99, *P*=0.059). G: Normalized head spine length of *D. lumholtzi* clone
202    TE exposed to *Gasterosteus aculeatus* after injection with eGFP-, dsIR25a- or dsIR93a-probe.
203    Predator exposure after eGFP-probe injection induces significant defense expression.
204    Individuals injected with dsIR25a- or dsIR93a-probe do not express defenses. In A, C, E, G
205    significant differences are indicated by letters. Groups sharing the same letter are not
206    significantly different (*P*>0.05). In B, D, E significant differences compared to the control are
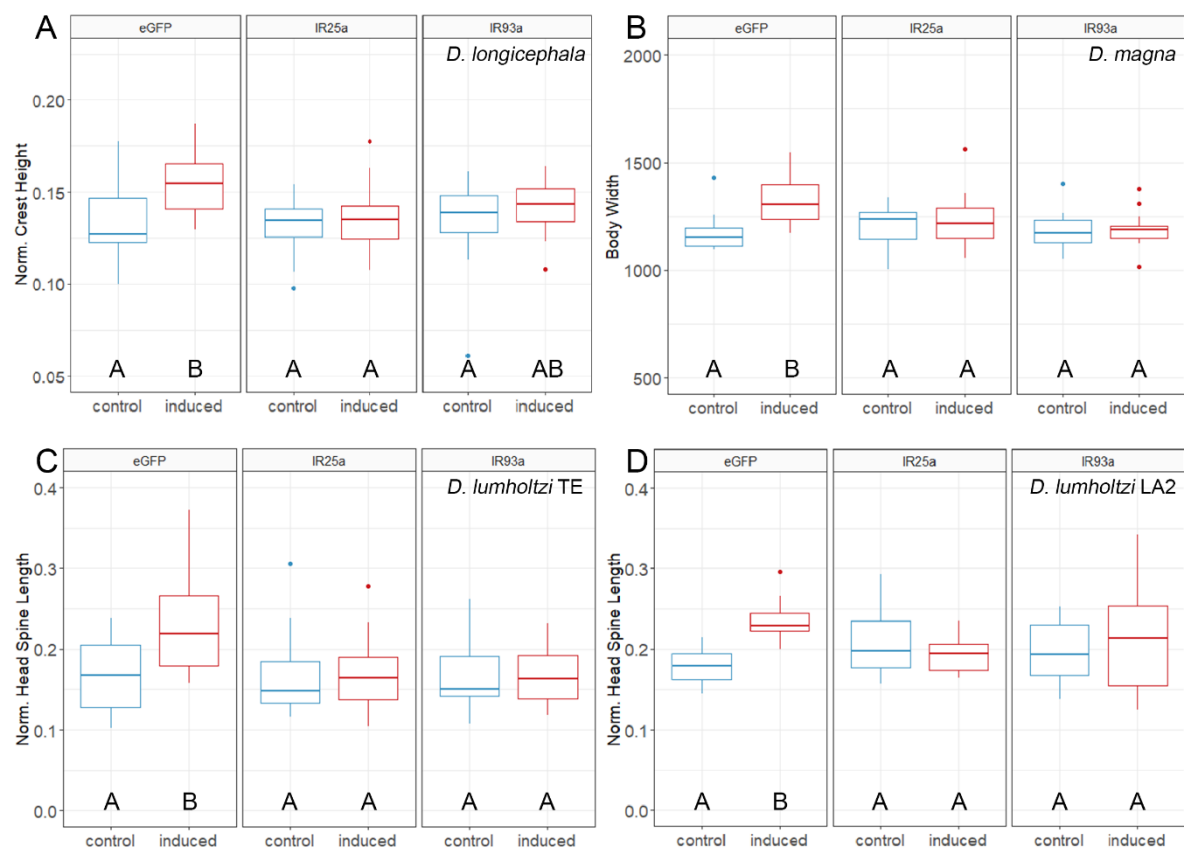207    indicated by asterisks (\**P*≤0.05, \*\* *P*≤0.01 tab. S1, S2).

208
209 **Figure 4:** Morphological defense expression after injection with the eGFP or the alternative
210 IR25a or IR93a dsRNA probes. A: In *D. longicephala*, normalized crest height is significantly
211 increased upon predator exposure after eGFP probe injection. Animals injected with one of the
212 target probes do not express crests. B: In *D. magna*, body width is significantly increased upon
213 predator exposure after eGFP probe injection. Animals injected with one of the target probes
214 do not express increased body width. C: In *D. lumholtzi* TE, normalized head spine length is
215 significantly increased upon predator exposure after eGFP probe injection. Animals injected
216 with one of the target probes do not express increased head spines. D: In *D. lumholtzi* LA2,
217 normalized head spine length is significantly increased upon predator exposure after eGFP
218 probe injection. Animals injected with one of the target probes do not express increased head
219 spines. Statistical results are listed in tables S5, S6
220

## Discussion

222 Our results provide a first view on the combinatorial expression patterns of these previously *in*

223 *silico* identified chemo-co-receptors in *Daphnia*.

224

225 **Co-receptor IR expression levels in the antennules**

226    A chemosensory function of the *Daphnia* antennules has already been demonstrated through

227    mechanical impairment of the antennules (Weiss, Leimann, and Tollrian 2015). However, the

228    chemoreceptors expressed by the antennules remained undetermined. We here report a higher

229    abundance of IR25a and IR93a mRNA in the antennules compared to the rest of the body. In

230    the swimming antennae, we observe a somewhat higher (~0.5 log2-fold) level of both co-

231    receptor IRs in comparison to the body. Based on these results, we also expect to find more

232    receptor protein molecules in the antennules than in swimming antennae and even less in the

233    body.

234    Comparing the degree of the expression levels of both receptors, the IR25a seems to be more

235    abundant in the antennules than the IR93a. In the swimming antennae both receptors seem

236    equally expressed. This further supports the idea that the antennules serve as a functional unit

237    of chemoreception. In different crustacean taxa, a high RNA expression level of the IR25a

238    coincides with the location of the IR25a protein on the lateral flagella (bearing the aesthetascs)

239    that mediate chemoreception (Tadesse et al. 2011; Stepanyan et al. 2004; Kozma, Ngo-Vu,

240    Rump, et al. 2020; Kozma et al. 2018; Kozma, Ngo-Vu, Yan Wong, et al. 2020; Corey et al.

241    2013; Groh-Lunow et al. 2015; Zbinden et al. 2017; Hollins et al. 2003). This implies that also

242    in the onchyuran *Daphnia* the IR25a and IR93a proteins are localized on the antennules and

243    potentially engage in the perception of chemical cues. To further support our observations,

244    antibody staining directed against IR25a and IR93a would be necessary. Unfortunately, the only

245    antibody that is currently available (product #EKY005, Kerafast USA), is directed against the

246    IR25a in lobster and gave unreliable staining patterns and Western Blot validation failed; a

247    similar effect was observed in salmon lice (Komisarczuk, Grotmol, and Nilsen 2017).

248    While we now have strong evidence that both co-IR proteins are located on the antennules, we

249    still know little about their specific localization in the body and the swimming antennae. In case

250    there are peripheral receptors expressed, these could either also be of chemosensory type, or

13

251    they could be thermo-sensitive as has been demonstrated when the IR25a or IR93a are co-

252    expressed with e.g. the IR21a in *Drosophila* (Ni 2021). These receptor classifications will be

253    tasks for future investigations.

254    As chemoreceptors are often subject to an increased turnover rate when being stimulated with

255    their ligands (Koerte et al. 2018), we investigated the effect of predatory chemical cues on

256    differential gene expression in a time dependent manner.

257

258    **Time dependent gene expression patterns of IR25a and IR93a**

259    We compared expression levels in the antennules of predator exposed to control

260    *D. longicephala*. Six hours post predator exposure we detect a significant upregulation of both

261    IRs. Together with the subsequent continuous upregulation of both receptors, this probably

262    marks the onset of an increased receptor turn-over rate which is due to ligand-receptor binding

263    activity (Koerte et al. 2018). It is important to mention that this does not depict the point in time

264    for the onset of predator perception. This must lie earlier, if not even instantaneous, as increased

265    cell proliferation patterns have been reported already two hours post predator exposure (Graeve

266    et al. under revision). Ecologically, predator detection resulting in the fast onset of the

267    mechanisms engaged in defense expression is critical. The longer the time lag between predator

268    perception and the onset of such mechanisms, the longer it takes for the defenses to serve as an

269    effective protection (Clark and Harvell 1992; Jeschke, Laforsch, and Tollrian 2008; Hoverman

270    and Relyea 2007; Gabriel et al. 2005).

271    In *Drosophila* such a ligand-dependent up-regulation in the IRs' mRNA expression levels has

272    not been reported (Koerte et al. 2018) and we therefore speculate differences in the receptors'

273    relevance for detecting chemical agents in these two taxa. *Drosophila* possesses a highly

274    divergent group of ORs whose mRNA expression levels change in response to ligands, but

275    these ORs are absent in *Daphnia*. Together with the findings reported by Kozma et al. 2020,

14

276    we hypothesized, that chemoreception in *Daphnia* is a central function of the IRs. To support

277    this idea, we tested the functional involvement of these co-IRs using RNAi.

278

279    **Functional analysis of IR25a and IR93a**

280    All results were reproducible with the alternative probes, targeting a different gene region.

281    Together with qPCR results, we detect a successful knock-down of our target genes in all

282    species. Injection of the eGFP control probe does not affect defense expression in any of the

283    tested species. However, when injected with the IR25a probe, the three *Daphnia* species lose

284    their ability to react to predators. All measured parameters are not significantly different from

285    the control animals but significantly different from the predator exposed animals, so that

286    defenses are not at all expressed. When injected with the IR93a probe defenses in *D. magna*

287    and the two *D. lumholtzi* clones, are again not at all expressed. Only, in *D. longicephala*

288    defenses are significantly reduced but do not reach the control level, indicating a smaller

289    involvement of the IR93a in the perception of *Notonecta* specific signaling cues.

290    This shows that both IRs are functionally involved in the perception of the here involved

291    predator specific chemical cues. Our observations could be explained by two scenarios 1.) The

292    IR25a and the IR93a assemble and function as one chemoreceptor unit. However, as this

293    receptor combination was shown to function as a cool sensor and detected in the periphery of

294    the chemosensory organs in *Drosophila,* we anticipate it to be unlikely to have chemosensory

295    abilities in *Daphnia* (Knecht et al. 2016). 2.). Each of the two IRs function as chemo-co-

296    receptors and assemble with respective tuning receptors to form functional chemoreceptor units.

297    This also explains why the chemosensory capacities i.e. in detecting and reacting to this range

298    of chemosensory signals are hampered, as the knock-down of both IRs impairs receptor

299    assembly and trafficking. Even though the chemical composition of the *Triops* and the

300    *Notonecta* specific signaling cues have not been elucidated, we are highly confident that they

301    are different in their nature, due to their phylogenetic distance and the distinct responses they

302    induce in the different prey species (reviewed in Weiss & Tollrian 2018). Further, bile salts are

303    specific to vertebrates and most likely not present in any invertebrate taxon (Hahn et al. 2020).

304    Together with the fact, that even the experimentally necessary environmental transfer induced

305    the differential expression of both receptors further supports their co-receptor function.

306    Interesting is that the knock-down of the IR93a in *D. longicephala* only reduces but not prevents

307    defense expression. This indicates that the perception of the cues associated with the *Notonecta*

308    kairomone are predominantly perceived via IR25a receptor functioning and to a less extent via

309    the IR93a. Future studies will aim to identify the concrete tuning IR(s) that assemble with the

310    here identified co-IRs mediating chemoreception of natural substances in the environment. This

311    also lays the fundamental basis for understanding how *Daphnia* is able to react to changes in

312    the chemical environment and adapt through phenotypic plasticity. With respect to sensory

313    ecology, knowing the involved receptors may also guide to disentangling chemical signaling

314    agents, whose chemical identification is often the search for the needle in the haystack. By this

315    we will be able to better understand organism-by-environment interactions and how this can

316    have an ecosystem-wide effect.

317

318    **Material and Methods**

319    ***Daphnia* cultures**

320    *Daphnia longicephala* clone LP1 (Lara-Pond, Australia) and *D. lumholtzi* clones LA2

321    (Louisiana, USA; kindly provided by Ramcharan) and TE (Fairfield Reservoir, Texas, USA;

322    kindly provided by Sterner) were cultured in artificial *Daphnia* medium (ADaM (Klüttgen et

323    al. 1994)) in 1 L beakers (Weck®, Germany) containing 20 - 25 age-synchronized individuals.

324    *D. magna* clone FT44-2 (Rockpool 44, Tvärminne, Finland, kindly provided by D. Ebert) was

325   cultured in charcoal-filtered tap water (to cohere with the culture conditions of *Triops*) in 1 L

326   beakers containing 10 to 15 age-synchronized individuals. Animals were kept under constant

327   day:night conditions (16 h:8 h) at $20 \pm 1°C$ and fed *ad libitum* with the algae *Acutodesmus*

328   *obliquus*. The beakers were cleaned every 48 hours to remove exuviae, debris and excess algae.

329   Half of the medium was exchanged weekly.

330

331   **Predator cultures**

332   Backswimmers (*Notonecta* spec.) were collected from the ponds of the Ruhr-University

333   Botanical Garden. Animals were maintained in 1 L beakers (WECK®, Germany) filled with

334   charcoal-filtered tap water under standardized conditions ($20 \pm 1°C$ with 16 h:8 h light:dark

335   cycle). They were fed *ad libitum* with *Daphnia* spec.. *Triops* spec. were raised from sand

336   containing the eggs. Animals were kept in 1 L plastic tanks filled with one part charcoal-filtered

337   tap water and one part pre-desalted water under standardized conditions ($20 \pm 1°C$ with 16 h:8 h

338   light:dark cycle). *Triops* spec. were fed daily with fish flakes (Futter Granulat, MultiFit) (flakes

339   were crushed for freshly hatched animals) and after reaching a body length of ~0.5 cm were fed

340   additionally with *Daphnia* spec..

341   Three-spined sticklebacks (*Gasterosteus aculeatus*) (Zoo Zajac, Duisburg, Germany) were

342   cultured in ADaM in a 60 L glass tank at a constant temperature of $20 \pm 1°C$ with 16 h:8 h

343   light:dark cycle. Fish were fed *ad libitum* every 24 h with living *Daphnia* spec. and frosted

344   *Chironomus* larvae (Amtra, Germany). All animals were kept under conditions complying with

345   care and welfare.

346

347   **RNAi-probe design and synthesis**

348   RNAi-probes were designed against transcriptomic data of *D. longicephala* and *D. lumholtzi*,

349   and     the     online     deposited     *D.     magna*     genome     data

17

350 (https://metazoa.ensembl.org/Daphnia_magna/Info/Index). Probes were cloned in-house

351 following the requirements and strategy published by (Knorr et al., 2013; Posnien et al., 2009,

352 , fig. 5). For reverse transcription of a ~500 bp probe, we designed primers in Primer3 (tab. 3):

353 Length: 19 – 22 bp; Max Self Complementary: 5; Max 3' Self Complementary: 1; Max Pair

354 End Complementary: 1. The desired annealing temperature was set to 60 °C. BLAST homology

355 search was performed for the whole probe sequence with settings optimized for ´somewhat

356 similar sequences` (blastn) to exclude off-targets.



357

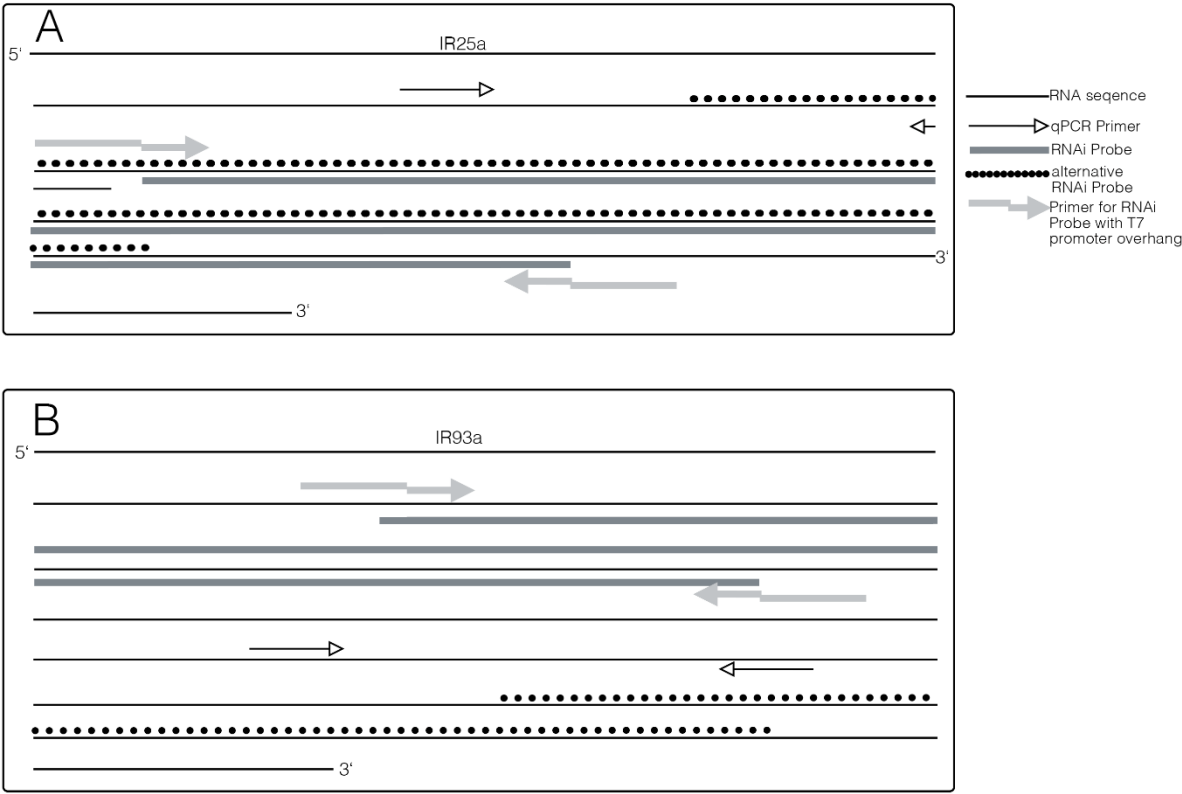358 **Figure 5:** Probe design. Extract of the IR25a (A) consensus and IR93a (B) obtained from the
359 sequences of *D. longicephala, D. magna* and *D. lumholtzi*. Displayed are the positions of the
360 qPCR primers (black arrow), the primers for our custom designed RNAi probe (grey arrow)
361 and the respective probe sequence (grey line) and the universal RNAi probe sequence (dotted
362 line).

363

364

365

18

366 **Tab. 3:** List of primers used to synthesize RNAi probes from cDNA and qPCR

| Gene Name | Primer Name | Sequence (5' – 3') | Explanation |
|---|---|---|---|
| IR25a with T7 promotor overhang | DLo_IR25a_RNAi_T7_fwd | **TAATACGACTCACTATAGG**ATACAAGGTCCAGTACGCGC | IR25a primer with T7 Promotor region (bold) to amplify IR25a from *D. longicephala* cDNA |
| | DLo_IR25a_RNAi_T7_rev2_2 | **TAATACGACTCACTATAGG**GTCGCCTACACAAACAAGCCA | |
| IR93a with T7 promotor overhang | DLo_IR93a_RNAi_T7_fwd3 | **TAATACGACTCACTATAGG**GTCCGCCAACGAGTCATCAAT | IR93a primer with T7 Promotor region (bold) to amplify IR93a from *D. longicephala* cDNA |
| | DLo_IR93a_RNAi_T7_rev3 | **TAATACGACTCACTATAGG**GGCGACCTGCAGTTATGGAAC | |
| qPCR primer for IR25a | universal_IR25a_qPCR_fwd | GGACGTTTAATTGCTGCCACTT | qPCR IR25a |
| | universal_IR25a_qPCR_rev | AGTTGACAAATCGTCCAGTGAGT | |
| qPCR primer for IR93a | universal_IR93a_qPCR_fwd | TTAGGTCAACGAGAAATGCCGA | qPCR IR93a |
| | universal_IR93a_qPCR_rev | TGGTGTAGGTCGGAAATGTCAG | |
| Tatabox binding protein | Dlo_tbp_fwd_1 | ACC TTG CCG GAA TAG TTG TG | *D. longicephala* reference gene |
| | Dlo_tbp_rev_1 | GAA TGC TGA AAC CAG GGC TA | |
| Carboxyl-terminal PDZ ligand of neuronal nitric oxide | Dlongi_CAPON_fdw2 | TTGCAGTTGATTGGCGAGGACA | *D. longicephala* reference gene |
| | Dlongi_CAPON_rev2 | ATGAAGAGTGGGCAGACTGGGA | |
| Tatabox binding protein | Dm_Tbp_fwd | GCAGGGAAGTTTAGTTTCTGG | *D. magna* reference gene |
| | Dm_Tbp_rev | TGGTATGCACAGGAGCAAAG | |
| Tatabox binding protein | Dlum_tbp_fwd_1 | ACCAGCAGATTTTGCCTCAC | *D. lumholtzi* reference gene |
| | Dlum_tbp_rev_1 | GAGGTGTGAATCCCGGTAAA | |

367

368 For subsequent *in vitro* transcription with T7 polymerase, T7 promotors were added via PCR

369 using GoTaq Master Mix (Promega) on *D. longicephala* cDNA. The obtained amplicon was

370 used for TA-cloning into a pCRII vector (TOPO TA Cloning kit, Invitrogen) and transformed

371 into TOP 10 *E. coli* (Invitrogen). After Midi-prep (Nucleo Bonda Xtra Column Filter kit,

372 Machery & Nagel) samples were Sanger-sequenced for validation. *In vitro* transcription was

373 conducted using the HiScribe T7 High Yield RNA Synthesis kit (New England Biolabs).

374 Finally, double-stranded RNA-probes (dsRNAi-probes) were cleaned using the Monarch RNA

375 clean-up kit (New England Biolabs, Germany).

376    As a negative control, we purchased an eGFP-probe as *Daphnia* do not have this sequence

377    encoded in the genome (Eupheria Biotech, Dresden, Germany; Sigma Product ID: EHUEGFP).

378    We validated our findings using probes that lie in a different region of the IR25a and IR93a

379    gene. In the case of the IR93a this alternative probe targets a region that does not overlap with

380    our initial probe. The IR25a sequence did not permit such an alternative non-overlapping probe,

381    and therefore, we generated a probe that overlaps with the other probe by 426 bp. These control

382    probes were also purchased from Eupheria Biotech (Dresden, Germany). All RNAi-probes

383    were diluted to a final concentration of 300 ng/µL in 4 µL aliquots and stored at -80 °C until

384    use. We further tested for sequence homology of the IR25a probe to the IR93a gene and vice

385    versa, yielding only weak homology. Sequence homology matrix between probes and target

386    sequence are given in table 4.

387

388    **Tab. 4:** Sequence homology between *IR25a* and *IR93a* consensus sequences obtained from *D. longicephala,*
389    *D. magna* and *D. lumholtzi* and injected RNAi probes. dsIR25a and dsIR93a probes are designed with
390    *D. longicephala* cDNA. The alternative RNAi probes targeting different sequence regions of the genes
391    "universal dsIR25a" and "universal dsIR93a" were designed for the consensus sequence of all three species.
392    Alignments were performed using the EMBL-EBI Multiple Sequence Alignment tool (Madeira et al. 2019).
393

| Gene \ Probe | dsIR25a | dsIR93a | alternative dsIR25a | alternative dsIR93a |
|---|---|---|---|---|
| *IR25a* | 92.26% | 65.40% | 100,00% | 61.94% |
| *IR93a* | 66.67% | 97.03% | 61.87% | 100,00% |

394

395

## Predator exposure bioassays

397    *D. longicephala* were exposed to *Notonecta* spec.. For that, we used a 12 L glass tank filled

398    with 4 L ADaM. Seven net cages (mesh size 150 µm), each containing one Notonectid were

399    placed into the tank. Predators were fed 10 adult *Daphnia* each. After 24 hours two Notonectids

400    were removed to avoid over-exposure and to create space for net cages with *D. longicephala*.

401    3-day old *D. longicephala* were added to the tanks in net cages containing a maximum of 20

402    *Daphnia* and fed *ad libitum* with *Acutodesmus obliquus* algae.

403   *D. magna* were exposed to *Triops* spec. in 12 L glass tanks filled with 3 L charcoal-filtered tap

404   water, a layer of approximately 0.5 cm sand and three *Triops* spec. (with <1 cm body length).

405   Predators were fed *ad libitum* with 3-day old *D. magna* and fish flakes. After 24 hours net cages

406   with 4-day old test specimens were added to the tank and fed *ad libitum* with *Acutodesmus*

407   *obliquus*.

408   To also exclude that are effects are of clonal origin, we also tested two clones of the same

409   species. We exposed *D. lumholtzi* clones TE and LA2 to *Gasterosteus aculeatus* in12 L glass

410   tanks filled with 8 L ADaM and two sticklebacks with a body length of 3 – 5 cm. After 24 h

411   net cages with 3-day old *D. lumholtzi* were added to the tank and fed *ad libitum* with

412   *Acutodesmus obliquus* algae.

413

414   **Controls for predator bioassays**

415   All controls were handling controls conducted at the same time with the same set of equipment

416   and liquid batches lacking just one variable: no predators were added to the tanks.

417

418   **Tissue specific sampling to determine IR25a and IR93a localization**

419   To determine co-receptor localization, we dissected three-day old *D. longicephala* in a tissue-

420   specific manner, removing the antennules (by cutting off the rostral tip), and swimming

421   antennae, which were dissected with metal tweezers. Antennules, swimming antennae and the

422   body were then transferred into tubes containing DNA/RNA shield (Zymo Research). Samples

423   were directly manually homogenized with plastic pistils and stored at -80 °C until further usage.

424   Each biological replicate contained 40-60 animals which we found to provide enough RNA for

425   quantitative PCR.

426

427 **Predator-induced differential gene expression levels of IR25a and IR93a in the**

428 **antennules.**

429 To investigate predator-induced differential IR gene expression, we exposed 40-60 three-day

430 old *D. longicephala* to *Notonecta* spec. as described in the induction assay for 0.5 h, 1 h, 2 h,

431 4 h, 6 h, 12 h, and 24 h. Subsequently, animals were killed, and antennules were cut off with a

432 sharp razor blade. Again, samples were homogenized and stored in DNA/RNA Shield™ (Zymo

433 Research, Germany) at -80 °C until further usage. Each biological replicate contained 40-60

434 animals providing good quality and quantity yields for gene expression analysis.

435

436 **Quantitative reverse transcription PCR (RT-qPCR)**

437 RNA for RT-qPCR was extracted with the Quick-RNA Microprep Kit (Zymo Research) and

438 diluted to a working concentration of 10 ng/μL. The Luna® One-Step RT qPCR Kit (New

439 England Biolabs, Germany) was used for RT-qPCR in the LightCycler® 96 System (Roche,

440 Germany) on 96 well plates (MJ white, Sarstedt, Germany) according to the protocol with a

441 modified total reaction volume of 10 μL. For each treatment, a minimum of three biological

442 and two technical replicates (from which we calculated the mean CT) were used. Primer

443 efficiency was calculated using LinReg PCR (Ruijter et al. 2009). All primers had an efficiency

444 of >0.87<1.0. We analyzed log2-fold expression changes based on the ddCT method (Livak

445 and Schmittgen 2001) with respect to primer efficiency using specific reference genes chosen

446 based on geNorm (Vandesompele et al. 2002) (tab. 5). Differential expression was determined

447 with a one-sample T-test on the log2-fold expression data.

448
449
450
451
452

**Tab. 5:** Validation of reference genes. **A:** Gene stability in *D. longicephala* antennules, 2nd antennae and body. Data of induced and control and injected and non-injected samples from all observed sampling points were used. **B:** Gene stability in *D. longicephala*. Data of injected (eGFP, dsIR25a or dsIR93a) and non-injected samples were used. **C:** Gene stability in *D. magna*. Data of injected (eGFP, dsIR25a or dsIR93a) and non-injected samples were used. **D:** Gene stability in *D. lumholtzi*. Data of injected (eGFP, dsIR25a or dsIR93a) and non-injected samples were used.

| specimen | gene | stability value |
|---|---|---|
| *D. longicephala* tissues | CAPON/tbp | 1.644 |
| | IR93a | 1.498 |
| | IR25a | 1.884 |
| *D. longicephala* | IR25a/CAPON | 0.43 |
| | IR93a | 0.524 |
| | tbp | 0.621 |
| *D. magna* | tbp/CYP | 0.202 |
| | IR25a | 0.29 |
| | IR93a | 0.393 |
| | GAPDH | 0.65 |
| *D. lumholtzi* | CAPON/tbp | 0.233 |
| | IR93a | 0.257 |
| | IR25a | 0.317 |

## Microinjection

For microinjections we used the FemtoJet 4i (Eppendorf) attached to a micromanipulator (Narishige). Capillaries (without filament, length: 100 mm, outer diameter: 1 mm, inner diameter: 0.58 mm, Hilgenberg, GmbH, Germany) were pulled using the Micropipette Puller P-1000 (Sutter Instruments) with the following settings: ramp = 505, heat = 500, pull = 40, velocity = 60, time = 120, pressure = 500. Phenol red was added in a ratio of 1:5 to the RNAi-probes for visual control of injection success. Probes were filled into the capillary using a fine glass pipet that was pulled out over an open flame. Filled injection capillaries were opened by breaking the tips with tweezers and sharpened over a wet stone. Just prior to injection the probes (300 ng/µl) were diluted with phenol red using a ratio of 1:5 to obtain visual control over the injection success. We validated that phenol red and eGFP do not affect *Daphnia* viability or their ability to express inducible defenses (fig. 6).

484  For the injection of the RNAi probes, we established a microinjection setup in which we

485  injected juvenile and adult *Daphnia* of the different species. For this we designed a Plexiglas

486  object slide (8 cm x 2.5 cm x 0.4 cm), containing u-shaped notches of 0.5 cm and 0.25 cm

487  diameter to fit the respective sizes of different *Daphnia* age and size classes (fig. 6 A). For

488  injection the *Daphnia* were held in place by placing the *Daphnia* backwards against the frame

489  of the notch (fig. 6 B, C, D). The injection needle was positioned on the head near the base of

490  the 2$^{nd}$ antenna (fig. 6 B, C, D). Injection pressure was set to 300 hPa, holding pressure was

491  30 hPa. *D. longicephala* were injected in the neck region near the base of the swimming

492  antenna, while *D. magna* and *D. lumholtzi* were injected through the underside of the rostrum.

493  The injection lasted 3-12 s until a red stain inside the *Daphnia* indicated the injection success.

494  Subsequently, the viable and injected *Daphnia* were transferred into snap-cap vials containing

495  100 ml ADaM, or kairomone enriched ADaM, respectively. We ensured that injected media

496  can also reach the cells of interest by injecting Hoechst as nuclear marker. This stained all body

497  cells including the cells at the base of the antennules (fig. 6 E, F).

498



499
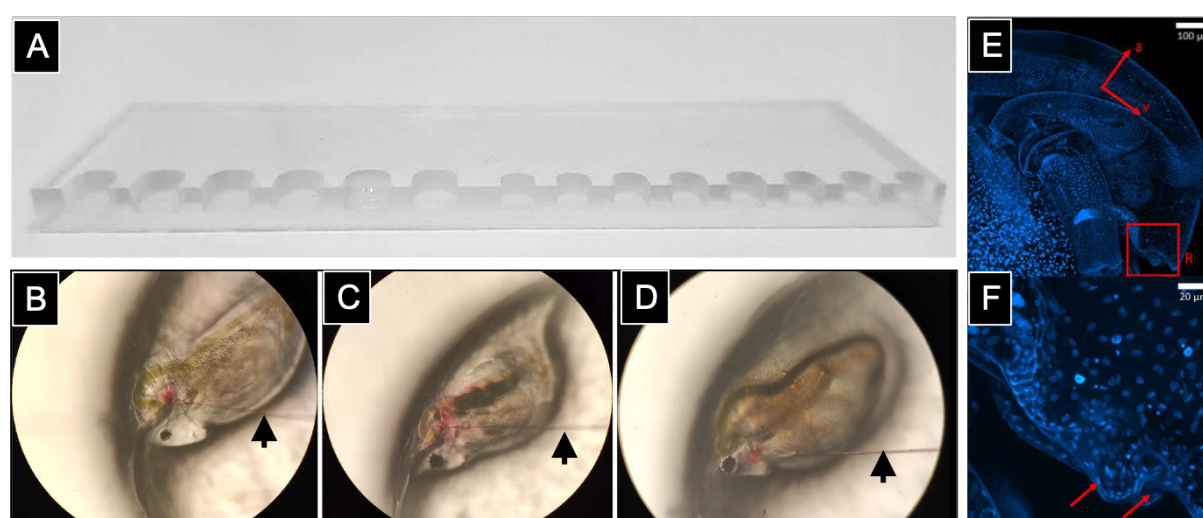500  **Figure 6:** Methodology used to inject RNAi probes in juvenile *Daphnia* **A**: custom designed
501  object slide holder with U-shaped notches to position the different *Daphnia* species during
502  microinjections. **B**: Example for microinjections performed with *D. longicephala*, using phenol
503  red as a visual guidance of successful injection **C**: Example for microinjections performed with

504  *D. lumholtzi*, and **D**: Example for microinjections performed with *D. magna*. **B-C**: Arrows mark
505  the injection needle. **E, F**: Display of Hoechst injected *D. magna*, where the microinjection of
506  the cell marker dye, successfully reaches and stains, cells of the head and especially the basis
507  of the antennules. Boxes mark the region of the antennules, red arrows depict sensory somata
508  at antennules' base.
509

510

511  **Functional assessment of IR25a and IR93a**

512  To study the function of the two putative co-receptors, we microinjected three-day old

513  *D. longicephala*, four-day old *D. magna* and three-day old *D. lumholtzi* (clone TE and LA2)

514  with the dsRNAi-probes. After 2 to 3 hours the animals were transferred to the respective

515  predator treatment. The phenotypes were then analyzed in the instar where defense expression

516  normally occurs, which is usually two molting cycles after predator exposure, so approximately

517  48 hours post predator exposure (fig. 7). We validated down-regulation of the target genes again

518  using qPCR. For this we collected 5*10 *D. longicephala*, 5*10 *D. lumholtzi* and 5*5 *D. magna*

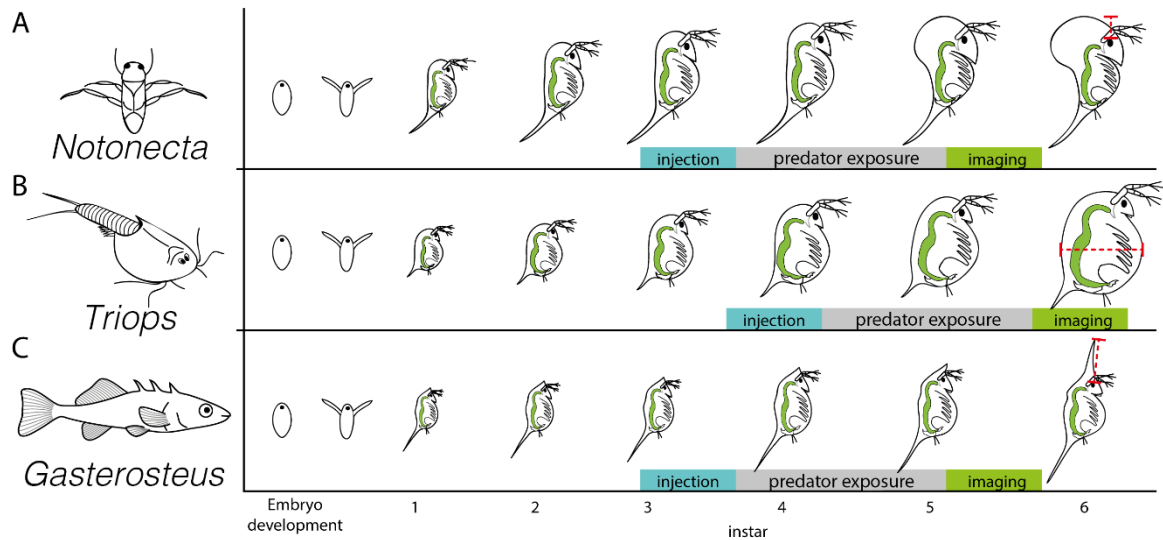519  4 to 6 h post microinjection in RNA shield.

520



521

522  **Figure 7: Schematic display of the experimental strategy used for RNAi**. **A:**
523  *D. longicephala* was microinjected with the respective RNAi probes once the animals reached

25

524    the third instar. After three hours the animals were transferred to the predator *Notonecta* or

525    control treatment respectively. Defense expression was measured as crest height in the fifth

526    instar. **B:** *D. magna* was injected with RNAi probes in the fourth instar. Three hours after

527    microinjection, the animals were transferred to the predator *Triops* or the control condition

528    respectively. Defense expression was measured as body width in the sixth instar. **C:** Both

529    *D. lumholtzi* clones LA2 and TE, were microinjected with both the respective RNAi probes in

530    the third juvenile instar and exposed to the predator *Gasterosteus aculeatus* two to three hours

531    later. Defense expression was measured as head spine length in the fifth instar.

532

533

534    **Morphological defense measurement**

535    Crest height in *D. longicephala* was measured in a vertical line from the upper margin of the

536    compound eye to the most distal point of the head. As this trait is correlated with the body size,

537    we normalized crest height by dividing crest height by body length. Body length was measured

538    from the upper margin of the compound eye to the root of the tail spine. Body width in *D. magna*

539    was measured in a horizontal line at the widest point of the body. Head spine length in *D.*

540    *lumholtzi* was measured from the upper margin of the compound eye to the tip of the head spine

541    and again normalized by body length as measured above (red lines in fig. 7). For measurements

542    we used an image analysis system composed of Olympus SZX16 stereo microscope equipped

543    with a digital camera (Olympus DP74) controlled by the software cell sense. Measurements

544    were taken on the images using the line tools.

545

546    **Data management and statistical analyses of morphological defenses and RNAi probe**

547    **injection effects**

548    All data was collected in Excel (Microsoft Inc.). We tested for normal distribution of the data

549    using a Shapiro-Wilk test. As the data for morphological defense expression after probe

550    injection did not follow a normal distribution, we log-transformed the data, which was then

551    normally distributed. To determine the effect of the injected probes, we used an analysis of

552   variance (ANOVA) with injected probe and treatment as factors. To determine differences

553   between individual groups analysis of variance was followed by a Bonferroni post hoc test.

554   Data is displayed untransformed. Statistical analyses and plots were made in R using the

555   ggplot2 package (R Development Core Team 2011; Hadley 2016).

556

557   **References**

558   Atema, Jelle. 1988. *Sensory Biology of Aquatic Animals*.

559   Benton, Richard. 2015. "Multigene Family Evolution: Perspectives from Insect Chemoreceptors."

560        *Trends in Ecology and Evolution*. https://doi.org/10.1016/j.tree.2015.07.009.

561   Benton, Richard, Kirsten S. Vannice, Carolina Gomez-Diaz, and Leslie B. Vosshall. 2009. "Variant

562        Ionotropic Glutamate Receptors as Chemosensory Receptors in Drosophila." *Cell* 136 (1): 149–

563        162. https://doi.org/10.1016/j.cell.2008.12.001.

564   Clark, C. W., and C. D. Harvell. 1992. "Inducible Defenses and the Allocation of Resources: A

565        Minimal Model." *American Naturalist*. 34 (4):543-551 https://doi.org/10.1086/285342.

566   Corey, Elizabeth A., Yuriy Bobkov, Kirill Ukhanov, and Barry W. Ache. 2013. "Ionotropic

567        Crustacean Olfactory Receptors." *PLoS ONE* 8 (4).

568        https://doi.org/10.1371/journal.pone.0060551.

569   Croset, Vincent, Raphael Rytz, Scott F. Cummins, Aidan Budd, David Brawand, Henrik Kaessmann,

570        Toby J. Gibson, and Richard Benton. 2010. "Ancient Protostome Origin of Chemosensory

571        Ionotropic Glutamate Receptors and the Evolution of Insect Taste and Olfaction." *PLoS*

572        *Genetics*. https://doi.org/10.1371/journal.pgen.1001064.

573   Derby, Charles D., Mihika T. Kozma, Adriano Senatore, and Manfred Schmidt. 2016. "Molecular

574        Mechanisms of Reception and Perireception in Crustacean Chemoreception: A Comparative

575        Review." *Chemical Senses* 41 (5): 381–98. https://doi.org/10.1093/chemse/bjw057.

576   Eyun, Seong Il, Ho Young Soh, Marijan Posavi, James B. Munro, Daniel S.T. Hughes, Shwetha C.

577        Murali, Jiaxin Qu, et al. 2017. "Evolutionary History of Chemosensory-Related Gene Families

578     across the Arthropoda." *Molecular Biology and Evolution*. 34(8):1838-1862

579     https://doi.org/10.1093/molbev/msx147.

580     Gabriel, Wilfried, Barney Luttbeg, Andrew Sih, and Ralph Tollrian. 2005. "Environmental Tolerance,

581     Heterogeneity, and the Evolution of Reversible Plastic Responses." *American Naturalist*.

582     166(3):339-353 https://doi.org/10.1086/432558.

583     Groh-Lunow, Katrin C., Merid N. Getahun, Ewald Grosse-Wilde, and Bill S. Hansson. 2015.

584     "Expression of Ionotropic Receptors in Terrestrial Hermit Crab's Olfactory Sensory Neurons."

585     *Frontiers in Cellular Neuroscience* 8 (FEB): 1–12. https://doi.org/10.3389/fncel.2014.00448.

586     Groh, Katrin C., Heiko Vogel, Marcus C. Stensmyr, Ewald Grosse-Wilde, and Bill S. Hansson. 2014.

587     "The Hermit Crab's Nose-Antennal Transcriptomics." *Frontiers in Neuroscience*.

588     https://doi.org/10.3389/fnins.2013.00266.

589     Hadley, Wickham. 2016. *Ggplot2: Elegrant Graphics for Data Analysis*. Springer.

590     Hahn, Meike Anika, Christoph Effertz, Laurent Bigler, and Eric Von Elert. 2019. "5A-Cyprinol

591     Sulfate, a Bile Salt From Fish, Induces Diel Vertical Migration in Daphnia." *ELife* 8 (Dvm): 1–

592     15. https://doi.org/10.7554/eLife.44791.

593     Hahn, Meike Anika, Eric von Elert. 2022. One fish kairomone and multiple effects in *Daphnia* species

594     - 5A-Cyprinol Sulfate induces morphological defenses in the invasive species *D. lumholtzi*.

595     Frontiers in Ecology & Evolution, https://doi.org/10.3389/fevo.2022.804521.

596     Hay, Mark E. 2009. "Marine Chemical Ecology: Chemical Signals and Cues Structure Marine

597     Populations, Communities, and Ecosystems." *Annual Review of Marine Science* 1 (1): 193–212.

598     https://doi.org/10.1146/annurev.marine.010908.163708.

599     Herzog, Quirin, and Christian Laforsch. 2013. "Modality Matters for the Expression of Inducible

600     Defenses: Introducing a Concept of Predator Modality." *BMC Biology* 11 (1): 113–23.

601     https://doi.org/10.1186/1741-7007-11-113.

602     Hollins, Bettye, Debra Hardin, Alexander A. Gimelbrant, and Timothy S. McClintock. 2003.

603     "Olfactory-Enriched Transcripts Are Cell-Specific Markers in the Lobster Olfactory Organ."

604     *Journal of Comparative Neurology*. 29(3):179-187. https://doi.org/10.1002/cne.10489.

605    Hoverman, Jason T., and Rick A. Relyea. 2007. "How Flexible Is Phenotypic Plasticity?

606        Developmental Windows for Trait Induction and Reversal." *Ecology* 88 (3): 693–705.

607        https://doi.org/10.1890/05-1697.

608    Jeschke, J. M., C. Laforsch, and R. Tollrian. 2008. "Animal Prey Defenses." In *Encyclopedia of*

609        *Ecology, Five-Volume Set*. https://doi.org/10.1016/B978-008045405-4.00858-2.

610    Joseph, Ryan M., and John R. Carlson. 2015. "*Drosophila* Chemoreceptors: A Molecular Interface

611        Between the Chemical World and the Brain." *Trends in Genetics*.31(12):683-695.

612        https://doi.org/10.1016/j.tig.2015.09.005.

613    Kenny, Nathan J., Xin Shen, Thomas T.H. Chan, Nicola W.Y. Wong, Ting Fung Chan, Ka Hou Chu,

614        Hon Ming Lam, and Jerome H.L. Hui. 2015. "Genome of the Rusty Millipede, *Trigoniulus*

615        *Corallinus,* Illuminates Diplopod, Myriapod, and Arthropod Evolution." *Genome Biology and*

616        *Evolution*. 7(5):1280-1295. https://doi.org/10.1093/gbe/evv070.

617    Knecht, Zachary A., Ana F. Silbering, Lina Ni, Mason Klein, Gonzalo Budelli, Rati Bell, Liliane

618        Abuin, et al. 2016. "Distinct Combinations of Variant Ionotropic Glutamate Receptors Mediate

619        Thermosensation and Hygrosensation in Drosophila." *ELife* 5: 1–15.

620        https://doi.org/10.7554/eLife.17879.

621    Knorr, Eileen, Linda Bingsohn, Michael R. Kanost, and Andreas Vilcinskas. 2013. "*Tribolium*

622        *Castaneum* as a Model for High-Throughput RNAi Screening." In *Advances in Biochemical*

623        *Engineering/Biotechnology*. https://doi.org/10.1007/10_2013_208.

624    Koerte, Sarah, Ian W. Keesey, Mohammed A. Khallaf, Lucas Cortés Llorca, Ewald Grosse-Wilde, Bill

625        S. Hansson, and Markus Knaden. 2018. "Evaluation of the DREAM Technique for a High-

626        Throughput Deorphanization of Chemosensory Receptors in Drosophila." *Frontiers in Molecular*

627        *Neuroscience* 11: 1–14. https://doi.org/10.3389/fnmol.2018.00366.

628    Komisarczuk, Anna Z., Sindre Grotmol, and Frank Nilsen. 2017. "Ionotropic Receptors Signal Host

629        Recognition in the Salmon Louse (*Lepeophtheirus Salmonis*, Copepoda)." *PLoS ONE* 12 (6): 1–

630        18. https://doi.org/10.1371/journal.pone.0178812.

631    Kozma, Mihika T., Hanh Ngo-Vu, Matthew T. Rump, Yuriy V. Bobkov, Barry W. Ache, and Charles

632    D. Derby. 2020. "Single Cell Transcriptomes Reveal Expression Patterns of Chemoreceptor

633    Genes in Olfactory Sensory Neurons of the Caribbean Spiny Lobster, *Panulirus Argus*." *BMC*

634    *Genomics* 21 (1): 1–19. https://doi.org/10.1186/s12864-020-07034-7.

635  Kozma, Mihika T., Hanh Ngo-Vu, Yuen Yan Wong, Neal S. Shukla, Shrikant D. Pawar, Adriano

636    Senatore, Manfred Schmidt, and Charles D. Derby. 2020. Comparison of Transcriptomes from

637    Two Chemosensory Organs in Four Decapod Crustaceans Reveals Hundreds of Candidate

638    Chemoreceptor Proteins. *PLoS ONE*. https://doi.org/10.1371/journal.pone.0230266.

639  Kozma, Mihika T., Manfred Schmidt, Hanh Ngo-Vu, Shea D. Sparks, Adriano Senatore, and Charles

640    D. Derby. 2018. "Chemoreceptor Proteins in the Caribbean Spiny Lobster, Panulirus Argus:

641    Expression of Ionotropic Receptors, Gustatory Receptors, and TRP Channels in Two

642    Chemosensory Organs and Brain." *PLoS ONE*, 2018.

643    https://doi.org/10.1371/journal.pone.0203935.

644  Livak, Kenneth J., and Thomas D. Schmittgen. 2001. "Analysis of Relative Gene Expression Data

645    Using Real-Time Quantitative PCR and the 2-ΔΔCT Method." *Methods*. 25(4):402-408.

646    https://doi.org/10.1006/meth.2001.1262.

647  Madeira, Fábio, Young Mi Park, Joon Lee, Nicola Buso, Tamer Gur, Nandana Madhusoodanan,

648    Prasad Basutkar, et al. 2019. "The EMBL-EBI Search and Sequence Analysis Tools APIs in

649    2019." *Nucleic Acids Research* 47 (W1): W636–41. https://doi.org/10.1093/nar/gkz268.

650  Ni, Lina. 2021. "The Structure and Function of Ionotropic Receptors in Drosophila." *Frontiers in*

651    *Molecular Neuroscience* 13 (February): 1–11. https://doi.org/10.3389/fnmol.2020.638839.

652  Núñez-Acuña, Gustavo, Cristian Gallardo-Escárate, Anne Berit Skiftesvik, David M. Fields, and

653    Howard I. Browman. 2019. "Silencing of Ionotropic Receptor 25a Decreases Chemosensory

654    Activity in the Salmon Louse *Lepeophtheirus Salmonis* during the Infective Stage." *Gene* 697

655    (October 2018): 35–39. https://doi.org/10.1016/j.gene.2019.02.012.

656  Pẽnalva-Arana, D. Carolina, Michael Lynch, and Hugh M. Robertson. 2009. "The Chemoreceptor

657    Genes of the Waterflea *Daphnia pulex*: Many Grs but No Ors." *BMC Evolutionary Biology* 9

658    (79). https://doi.org/10.1186/1471-2148-9-79.

659   Pijanowska, Joanna, Magdalena Markowska, Anna Ruszczyńska, Ewa Bulska, Piotr Dawidowicz,

660        Mirosław Ślusarczyk, and Magdalena Biesaga. 2020. "Kairomone-like Activity of Bile and Bile

661        Components: A Step towards Revealing the Chemical Nature of Fish Kairomone." *Scientific

662        Reports* 10 (1): 1–11. https://doi.org/10.1038/s41598-020-63456-z.

663   Pohnert, Georg, Michael Steinke, and Ralph Tollrian. 2007. "Chemical Cues, Defence Metabolites and

664        the Shaping of Pelagic Interspecific Interactions." *Trends in Ecology and Evolution*.

665        https://doi.org/10.1016/j.tree.2007.01.005.

666   Posnien, Nico, Johannes Schinko, Daniela Grossmann, Teresa D. Shippy, Barbora Konopova, and

667        Gregor Bucher. 2009. "RNAi in the Red Flour Beetle (*Tribolium*)." *Cold Spring Harbor

668        Protocols* 4 (8). https://doi.org/10.1101/pdb.prot5256.

669   R Development Core Team, R. 2011. *R: A Language and Environment for Statistical Computing. R

670        Foundation for Statistical Computing*. https://doi.org/10.1007/978-3-540-74686-7.

671   Rabus, Max, and Christian Laforsch. 2011. "Growing Large and Bulky in the Presence of the Enemy:

672        *Daphnia magna* Gradually Switches the Mode of Inducible Morphological Defences."

673        *Functional Ecology*. https://doi.org/10.1111/j.1365-2435.2011.01840.x.

674   Ringelberg, Joop. 2010. *Diel Vertical Migration of Zooplankton in Lakes and Oceans. (Springer)*.

675        Dordrecht: Springer Netherlands. https://doi.org/10.1007/978-90-481-3093-1.

676   Robertson, Hugh M. 2015. "The Insect Chemoreceptor Superfamily Is Ancient in Animals." *Chemical

677        Senses*. https://doi.org/10.1093/chemse/bjv046.

678   Ruijter, J. M., C. Ramakers, W. M.H. Hoogaars, Y. Karlen, O. Bakker, M. J.B. van den hoff, and A.

679        F.M. Moorman. 2009. "Amplification Efficiency: Linking Baseline and Bias in the Analysis of

680        Quantitative PCR Data." *Nucleic Acids Research*. https://doi.org/10.1093/nar/gkp045.

681   Rytz, Raphael, Vincent Croset, and Richard Benton. 2013. "Ionotropic Receptors (IRs):

682        Chemosensory Ionotropic Glutamate Receptors in *Drosophila* and Beyond." *Insect Biochemistry

683        and Molecular Biology* 43 (9): 888–97. https://doi.org/10.1016/j.ibmb.2013.02.007.

684   Selander, E, J Kubanek, M Hamberg, M X Andersson, G Cervin, and H Pavia. 2015. "Predator Lipids

685        Induce Paralytic Shellfish Toxins in Bloom-Forming Algae." *Proc Natl Acad Sci USA* 112 (20):

686    6395–6400. https://doi.org/10.1073/pnas.1420154112.

687    Stepanyan, Ruben, Bettye Hollins, S. Erin Brock, and Timothy S. McClintock. 2004. "Primary Culture

688    of Lobster (*Homarus Americanus)* Olfactory Sensory Neurons." *Chemical Senses*.

689    https://doi.org/10.1093/chemse/bjh023.

690    Tadesse, Tizeta, Manfred Schmidt, William W. Walthall, Phang C. Tai, and Charles D. Derby. 2011.

691    "Distribution and Function of Splash, an Achaete-Scute Homolog in the Adult Olfactory Organ

692    of the Caribbean Spiny Lobster *Panulirus Argus*." *Developmental Neurobiology*.

693    https://doi.org/10.1002/dneu.20862.

694    Tollrian, R, and C D Harvell. 1999. *The Ecology and Evolution of Induced Defenses*. *Functional*

695    *Ecology*. https://doi.org//j.1365-2435.2010.01789.x.

696    Vandesompele, Jo, Katleen De Preter, Filip Pattyn, Bruce Poppe, Nadine Van Roy, Anne De Paepe,

697    and Frank Speleman. 2002. "Accurate Normalization of Real-Time Quantitative RT-PCR Data

698    by Geometric Averaging of Multiple Internal Control Genes." *Genome Biology* 3 (7):

699    research0034.1. https://doi.org/10.1186/gb-2002-3-7-research0034.

700    Weiss, Linda C., Bauke Albada, Sina M. Becker, Sven W. Meckelmann, Julia Klein, Martin Meyer,

701    Oliver J. Schmitz, et al. 2018. "Identification of *Chaoborus* Kairomone Chemicals That Induce

702    Defences in *Daphnia*." *Nature Chemical Biology* 14 (12): 1133–39.

703    https://doi.org/10.1038/s41589-018-0164-7.

704    Weiss, Linda C., Julian Leimann, and Ralph Tollrian. 2015. "Predator-Induced Defences in *Daphnia*

705    *longicephala*: Location of Kairomone Receptors and Timeline of Sensitive Phases to Trait

706    Formation." *Journal of Experimental Biology* 218 (18): 2918–26.

707    https://doi.org/10.1242/jeb.124552.

708    Weiss, Linda C., and Ralph Tollrian. 2018. "Inducible Defenses in Crustacea." In *The Natural History*

709    *of the Crustacea, Life Histories, Volume 5*.

710    Wisenden, Brian D. 2000. "Olfactory Assessment of Predation Risk in the Aquatic Environment."

711    *Philosophical Transactions of the Royal Society B: Biological Sciences* 355 (1401): 1205–8.

712    https://doi.org/10.1098/rstb.2000.0668.

713    Yasumoto, Ko, Akinori Nishigami, Mina Yasumoto, Fumie Kasai, Yasuhiro Okada, Takenori Kusumi,

714         and Takashi Ooi. 2005. "Aliphatic Sulfates Released from Daphnia Induce Morphological

715         Defense of Phytoplankton: Isolation and Synthesis of Kairomones." *Tetrahedron Letters* 46 (28):

716         4765–67. https://doi.org/10.1016/j.tetlet.2005.05.027.

717    Zbinden, Magali, Camille Berthod, Nicolas Montagné, Julia Machon, Nelly Léger, Thomas

718         Chertemps, Nicolas Rabet, Bruce Shillito, and Juliette Ravaux. 2017. "Comparative Study of

719         Chemosensory Organs of Shrimp from Hydrothermal Vent and Coastal Environments."

720         *Chemical Senses*. 42(4):319-331. https://doi.org/10.1093/chemse/bjx007.

721    Zufall, Frank, and Steven D. Munger. 2016. Chemosensory Transduction: The Detection of Odors,

722         Tastes, and Other Chemostimuli. Chemosensory Transduction: The Detection of Odors, Tastes,

723         and Other Chemostimuli. https://doi.org/10.1016/C2014-0-00871-4.

724

725

## Supplementary Material

727

728



729

730
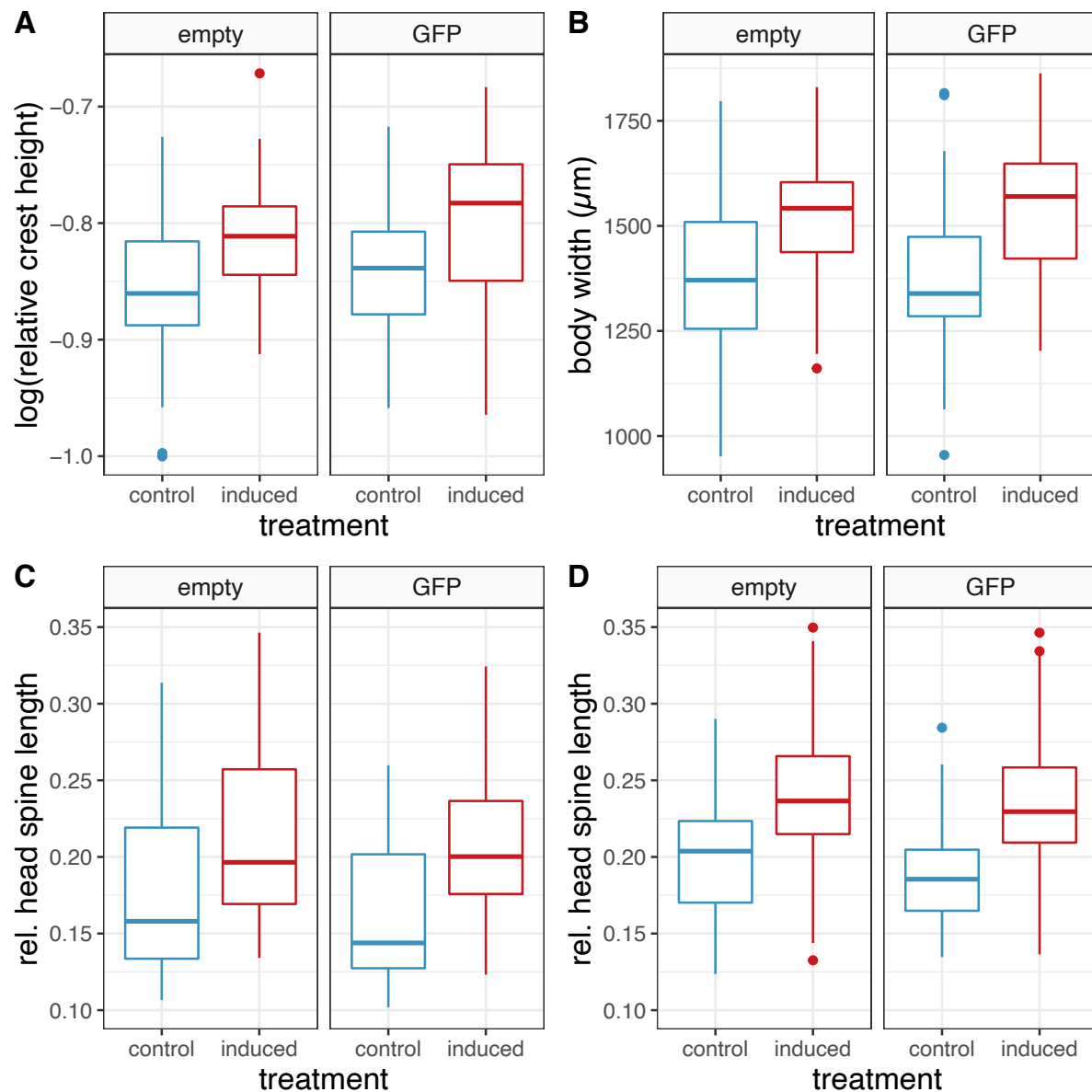
**Figure S1.: e**GFP dsRNA probe injection does not affect the expression of morphological defenses in **A:** *D. longicephala* significantly expresses crests: $ANOVA_{treatment}$ F(1, 0.11)=37.490; p<0.001, which is unaffected by the dsGFP RNA probe injection $ANOVA_{injection}$ F(1, 0.01)=3.281; p0=0.07 **B:** *D. magna* significantly expresses deeper bodies: $ANOVA_{treatment}$ F(1, 176229)=79.233; p<0.001, which is not affected by dsGFP probe injection $ANOVA_{injection}$ F(1, 4327)=0.195, p=0.659 **C:** *D. lumholtzi* TE significantly expresses head spines: $ANOVA_{treatment}$ F(1, 0.11894)=38.112; p<0.001, which is unaffected by dsGFP RNA probe injection: $ANOVA_{injection}$ F(1, 0.00791)=2.534, p=0.113 and **D:** *D. lumholtzi* LA2 significantly expresses head spines: $ANOVA_{treatment}$ F(1, 0.15336)=78.405; p<0.001, which is unaffected by dsGFP probe injection $ANOVA_{injection}$ F(1, 0.0048)=2.46, p=0.118

740

741

## Statistical results of RNAi knock down

743

744 **Table S1:** Factorial ANOVA on log(normalized crest height) in *D. longicephala*, log(body
745 width) in *D. magna* and log(normalized head spine length) in *D. lumholtzi* clones TE and LA2
746 after injection with eGFP-, dsIR25a- or dsIR93a-probe measured after 48 hours predator
747 exposure or control treatment. Related to fig. 5. Abbreviations: SS, square sum; MS, mean square.

| | SS | Degree of Freedom | MS | F | *P* | Partial eta-squared | Non-centrality | Observed power |
|---|---|---|---|---|---|---|---|---|
| *Daphnia longicephala* | | | | | | | | |
| Intercept | 219.66 | 1 | 219.66 | 81025.21 | ≤0.001 | 1.00 | 81025.21 | 1.00 |
| Injection | 0.01 | 2 | 0.01 | 2.74 | 0.066 | 0.02 | 5.49 | 0.54 |
| Treatment | 0.05 | 1 | 0.05 | 16.78 | ≤0.001 | 0.05 | 16.78 | 0.98 |
| Injection*Treatment | 0.02 | 2 | 0.01 | 3.56 | 0.029 | 0.02 | 7.13 | 0.66 |
| Error | 0.86 | 317 | 0.00 | | | | | |
| *Daphnia magna* | | | | | | | | |
| Intercept | 3027.82 | 1 | 3027.82 | 1482460.91 | ≤0.001 | 1.00 | 1482460.91 | 1.00 |
| Injection | 0.05 | 2 | 0.03 | 13.13 | ≤0.001 | 0.07 | 26.25 | 1.00 |
| Treatment | 0.06 | 1 | 0.06 | 31.46 | ≤0.001 | 0.09 | 31.46 | 1.00 |
| Injection*Treatment | 0.02 | 2 | 0.01 | 5.87 | 0.003 | 0.03 | 11.73 | 0.87 |
| Error | 0.690 | 338 | 0.00 | | | | | |
| *Daphnia lumholtzi* clone TE | | | | | | | | |
| Intercept | 150.76 | 1 | 150.76 | 12870.64 | ≤0.001 | 0.98 | 12870.64 | 1.00 |
| Injection | 0.21 | 2 | 0.10 | 8.76 | ≤0.001 | 0.07 | 17.53 | 0.97 |
| Treatment | 0.11 | 1 | 0.11 | 9.36 | 0.002 | 0.04 | 9.36 | 0.86 |
| Injection*Treatment | 0.16 | 2 | 0.08 | 6.80 | ≤0.001 | 0.05 | 13.61 | 0.92 |
| Error | 2.823 | 241 | 0.01 | | | | | |
| *Daphnia lumholtzi* clone LA2 | | | | | | | | |
| Intercept | 109.99 | 1 | 109.99 | 13966.74 | ≤0.001 | 0.98 | 13966.74 | 1.00 |
| Injection | 0.01 | 2 | 0.01 | 0.65 | 0.523 | 0.01 | 1.30 | 0.16 |
| Treatment | 0.09 | 1 | 0.09 | 11.57 | ≤0.001 | 0.05 | 11.57 | 0.92 |
| Injection*Treatment | 0.15 | 2 | 0.08 | 9.70 | ≤0.001 | 0.07 | 19.39 | 0.98 |
| Error | 1.929 | 245 | 0.01 | | | | | |

748

749 **Table S2:** Post hoc Bonferroni analysis on log(normalized crest height) in *D. longicephala*,
750 log(body width) in *D. magna* and log(normalized head spine length) in *D. lumholtzi* clones TE
751 and LA2 after injection with eGFP-, dsIR25a- or dsIR93a-probe measured after 48 hours
752 predator exposure or control treatment. Related to fig. 5.

| Injection / Treatment | | eGFP | | dsIR25a | | dsIR93a | |
|---|---|---|---|---|---|---|---|
| | | control | predator exposed | control | predator exposed | control | predator exposed |
| *Daphnia longicephala* | | | | | | | |
| eGFP | control | | ≤0.001 | n.s. | n.s. | n.s. | 0.175 |

| gene | condition | | | | | | |
|---|---|---|---|---|---|---|---|
| | predator exposed | ≤0.001 | | ≤0.001 | 0.015 | 0.016 | 0.613 |
| dsIR25a | control | n.s. | ≤0.001 | | n.s. | n.s. | 0.269 |
| | predator exposed | n.s. | 0.015 | n.s. | | n.s. | n.s. |
| dsIR93a | control | n.s. | 0.016 | n.s. | n.s. | | n.s. |
| | predator exposed | 0.175 | 0.613 | 0.269 | n.s. | n.s. | |
| *Daphnia magna* | | | | | | | |
| eGFP | control | | ≤0.001 | n.s. | n.s. | n.s. | 0.677 |
| | predator exposed | ≤0.001 | | ≤0.001 | ≤0.001 | ≤0.001 | ≤0.001 |
| dsIR25a | control | n.s. | ≤0.001 | | n.s. | n.s. | 0.053 |
| | predator exposed | n.s. | ≤0.001 | n.s. | | n.s. | n.s. |
| dsIR93a | control | n.s. | ≤0.001 | n.s. | n.s. | | 0.921 |
| | predator exposed | 0.677 | ≤0.001 | 0.053 | n.s. | 0.921 | |
| *Daphnia lumholtzi* clone TE | | | | | | | |
| eGFP | control | | ≤0.001 | n.s. | n.s. | n.s. | n.s. |
| | predator exposed | ≤0.001 | | ≤0.001 | ≤0.001 | ≤0.001 | 0.003 |
| dsIR25a | control | n.s. | ≤0.001 | | n.s. | n.s. | n.s. |
| | predator exposed | n.s. | ≤0.001 | n.s. | | n.s. | n.s. |
| dsIR93a | control | n.s. | ≤0.001 | n.s. | n.s. | | n.s. |
| | predator exposed | n.s. | 0.003 | n.s. | n.s. | n.s. | |
| *Daphnia lumholtzi* clone LA2 | | | | | | | |
| eGFP | control | | ≤0.001 | n.s. | 0.239 | 0.692 | 0.495 |
| | predator exposed | ≤0.001 | | 0.007 | 0.035 | 0.013 | 0.003 |
| dsIR25a | control | n.s. | 0.007 | | n.s. | n.s. | n.s. |
| | predator exposed | 0.239 | 0.035 | n.s. | | n.s. | n.s. |
| dsIR93a | control | 0.692 | 0.013 | n.s. | n.s. | | n.s. |
| | predator exposed | 0.495 | 0.003 | n.s. | n.s. | n.s. | |

753

754 **Table S3:** Differential gene expression statistical analysis results after probe injection as
755 displayed in in fig. 5.

| species | gene | mean | T-value | *P*-value |
|---|---|---|---|---|
| *D. longicephala* | IR25a | -0.77 | -2.05 | 0.039 |
| *D. longicephala* | IR93a | -0.55 | -4.6 | 0.022 |
| *D. magna* | IR25a | -0.44 | -2.4 | 0.037 |
| *D. magna* | IR93a | -0.96 | -2.79 | 0.025 |

| | | | | |
|---|---|---|---|---|
| *D. lumholtzi* | IR25a | -0.35 | -4.4 | 0.006 |
| *D. lumholtzi* | IR93a | -0.35 | -1.99 | 0.059 |

756

757

758

759 **Table S4:** Factorial ANOVA on log(normalized crest height) in *D. longicephala*, log(body
760 width) in *D. magna* and log(normalized head spine length) in *D. lumholtzi* clones TE and LA2
761 after injection with eGFP or the alternative IR25a or IR93a dsRNA probes measured after
762 48 hours predator exposure or control treatment. Related to fig. S5. Abbreviations: SS, square sum;
763 MS, mean square

764

| | SS | Degree of Freedom | MS | F | *P* |
|---|---|---|---|---|---|
| *Daphnia longicephala* | | | | | |
| Intercept | 123.18 | 1 | 123.18 | 40476.56 | ≤0.001 |
| Injection | 0.02 | 2 | 0.01 | 3.48 | 0.033 |
| Treatment | 0.05 | 1 | 0.05 | 16.21 | ≤0.001 |
| Injection*Treatment | 0.02 | 2 | 0.01 | 3.87 | 0.023 |
| Error | 0.49 | 161 | 0.00 | | |
| *Daphnia magna* | | | | | |
| Intercept | 804.78 | 1 | 804.78 | 598880.90 | ≤0.001 |
| Injection | 0.01 | 2 | 0.00 | 2.22 | 0.115 |
| Treatment | 0.01 | 1 | 0.01 | 6.82 | 0.011 |
| Injection*Treatment | 0.01 | 2 | 0.01 | 4.21 | 0.018 |
| Error | 0.106 | 79 | 0.00 | | |
| *Daphnia lumholtzi* clone TE | | | | | |
| Intercept | 86.78 | 1 | 86.78 | 8035.48 | ≤0.001 |
| Injection | 0.15 | 2 | 0.08 | 6.98 | 0.001 |
| Treatment | 0.11 | 1 | 0.11 | 9.93 | 0.002 |
| Injection*Treatment | 0.15 | 2 | 0.08 | 7.11 | 0.001 |
| Error | 1.533 | 142 | 0.01 | | |
| *Daphnia lumholtzi* clone LA2 | | | | | |
| Intercept | 35.21 | 1 | 35.21 | 5320.24 | ≤0.001 |
| Injection | 0.00 | 2 | 0.00 | 0.31 | 0.737 |
| Treatment | 0.03 | 1 | 0.03 | 4.03 | 0.048 |
| Injection*Treatment | 0.06 | 2 | 0.03 | 4.47 | 0.015 |
| Error | 0.470 | 71 | 0.01 | | |

765

766

767 **Table S5:** Post hoc Bonferroni analysis on log(normalized crest height) in *D. longicephala*,
768 log(body width) in *D. magna* and log(normalized head spine length) in *D. lumholtzi* clones TE
769 and LA2 after injection with eGFP-, dsIR25a- or dsIR93a-probe measured after 48 hours
770 predator exposure or control treatment. Related to fig. S5.

771

| | eGFP | dsIR25a | dsIR93a |
|---|---|---|---|

| Injection | Treatment | control | predator exposed | control | predator exposed | control | predator exposed |
|---|---|---|---|---|---|---|---|
| *Daphnia longicephala* | | | | | | | |
| eGFP | control | | ≤0.001 | n.s. | n.s. | n.s. | 0.398 |
| | predator exposed | ≤0.001 | | ≤0.001 | ≤0.001 | ≤0.001 | 0.206 |
| dsIR25a | control | n.s. | ≤0.001 | | n.s. | n.s. | 0.316 |
| | predator exposed | n.s. | ≤0.001 | n.s. | | n.s. | n.s. |
| dsIR93a | control | n.s. | ≤0.001 | n.s. | n.s. | | n.s. |
| | predator exposed | 0.398 | 0.206 | 0.316 | n.s. | n.s. | |
| *Daphnia magna* | | | | | | | |
| eGFP | control | | 0.002 | n.s. | n.s. | n.s. | n.s. |
| | predator exposed | 0.002 | | 0.031 | 0.140 | 0.012 | 0.018 |
| dsIR25a | control | n.s. | 0.031 | | n.s. | n.s. | n.s. |
| | predator exposed | n.s. | 0.140 | n.s. | | n.s. | n.s. |
| dsIR93a | control | n.s. | 0.012 | n.s. | n.s. | | n.s. |
| | predator exposed | n.s. | 0.018 | n.s. | n.s. | n.s. | |
| *Daphnia lumholtzi* clone TE | | | | | | | |
| eGFP | control | | ≤0.001 | n.s. | n.s. | n.s. | n.s. |
| | predator exposed | ≤0.001 | | ≤0.001 | ≤0.001 | ≤0.001 | ≤0.001 |
| dsIR25a | control | n.s. | ≤0.001 | | n.s. | n.s. | n.s. |
| | predator exposed | n.s. | ≤0.001 | n.s. | | n.s. | n.s. |
| dsIR93a | control | n.s. | ≤0.001 | n.s. | n.s. | | n.s. |
| | predator exposed | n.s. | ≤0.001 | n.s. | n.s. | n.s. | |
| *Daphnia lumholtzi* clone LA2 | | | | | | | |
| eGFP | control | | 0.030 | n.s. | n.s. | n.s. | n.s. |
| | predator exposed | 0.030 | | n.s. | 0.269 | 0.182 | n.s. |
| dsIR25a | control | n.s. | n.s. | | n.s. | n.s. | n.s. |
| | predator exposed | n.s. | 0.269 | n.s. | | n.s. | n.s. |
| dsIR93a | control | n.s. | 0.182 | n.s. | n.s. | | n.s. |
| | predator exposed | n.s. | n.s. | n.s. | n.s. | n.s. | |

772

773

774